

The 1-point PDF of the Initial Conditions of our Local Universe from the IRAS PSC redshift catalogue

P. Monaco^{1,2}, G. Efstathiou², S. J. Maddox², E. Branchini³,
 C. S. Frenk⁴, R. G. McMahon², S. J. Oliver⁵, M. Rowan-Robinson⁵,
 W. Saunders⁶, W. J. Sutherland⁷, H. Tadros⁷, S. D. M. White⁸

¹*Dipartimento di Astronomia, Università di Trieste, via Tiepolo 11, 34131 Trieste, Italy*

²*Institute of Astronomy, Madingley Road, Cambridge CB3 0HA, UK*

³*Kapteyn Sterrewacht, Rijksuniversiteit Groningen, Postbus 800, 9700, AV Groningen, The Netherlands*

⁴*Department of Physics, University of Durham, DH1 3LE, UK*

⁵*Blackett Laboratory, Imperial College, Prince Consort Road, London SW7 2BZ, UK*

⁶*Institute for Astronomy, Blackford Hill, Edinburgh EH9 3RJ, UK*

⁷*Nuclear and Astrophysics Laboratory, Keble Road, Oxford OX1 3RH, UK*

⁸*MPI-Astrophysik, Karl-Schwarzschild-Strasse 1, Garching bei Munchen, Germany D-85740*

Received 2000

ABSTRACT

The algorithm ZTRACE of Monaco & Efstathiou (1999) is applied to the IRAS PSCz catalogue to reconstruct the initial conditions of our local Universe with a resolution down to $\sim 5 h^{-1}$ Mpc. The 1-point PDF of the reconstructed initial conditions is consistent with the assumptions that (i) IRAS galaxies trace mass on scales of $\sim 5 h^{-1}$ Mpc, and (ii) the statistics of primordial density fluctuations is Gaussian. We use simulated PSCz catalogues, constructed from N-body simulations with Gaussian initial conditions, to show that local non-linear bias can cause the recovered initial PDF (assuming no bias) to be non-Gaussian. However, for plausible bias models, the distortions of the recovered PDF would be difficult to detect using the volume finely sampled by the PSCz catalogue. So, for Gaussian initial conditions, a range of bias models remain compatible with our PSCz reconstruction results.

Key words: Cosmology: theory – large-scale structure of the Universe – galaxies: distances and redshifts, clustering

1 INTRODUCTION

In the gravitational instability scenario, the large-scale structure of the Universe is formed by the growth of small fluctuations superimposed on a homogeneous background. In most inflationary models, these fluctuations are usually predicted to follow Gaussian statistics (see, e.g., Linde, 1990). Non-Gaussian initial conditions are however predicted by models based on topological defects (see, e.g., Brandenberger 1998), as well as by some inflationary models (see, e.g., Salopek 1999). At the present time, perturbations at galactic or smaller scales are highly non-linear, while the large-scale distribution of galaxies is still in the linear or mildly non-linear regime. For these fluctuations, the mapping of the mass distribution from the final to the initial configuration is single-valued. The gravitational evolution of the matter field can be inverted, even though at relatively small scales the evolution is beyond the linear stage

and strong non-Gaussian features in the density field are already present.

Under the assumption that galaxies trace the large-scale distribution of mass in a specified way, it is possible to recover the initial perturbation field which has given rise to the observed galaxy distribution. It is interesting to try to recover the initial conditions of our local Universe, not simply for understanding our local cosmography, but for other reasons as well. The inversion itself does not require any assumption concerning the detailed statistical properties of the density field. A reconstruction of initial conditions can therefore be used to test the assumption of Gaussianity. Furthermore, it can be used in N-body simulations to mimic the growth of clustering in our local Universe. This type of simulations have many uses, e.g. to produce predictions of our local peculiar velocity field, to quantify Malmquist biases in peculiar velocity measurements etc. (see, e.g., Kolatt et al, 1996; Narayanan et al. 1999).

The reconstruction of initial conditions is hampered by the well-known facts that galaxies are biased tracers of the matter density, and that the details of this bias are poorly known (see, e.g., Tegmark & Peebles 1998; Catelan et al. 1998; Lahav & Dekel 1999; Pearce et al. 1999; Benson et al. 1999; Somerville et al. 1999; Seljak 2000; Sigad, Branchini & Dekel 2000). A model-independent inclusion of bias in a reconstruction algorithm is not possible at present. Besides, for initial Gaussian perturbations the non-Gaussian statistics of the matter density field is determined by gravitational evolution. Galaxy bias influences the statistics of the galaxy density field. A reconstruction procedure applied to a biased galaxy density field but performed assuming no bias can correct only for gravitationally induced non-Gaussianities, thus letting bias induce non-Gaussian features in the recovered initial conditions. In other words, there is a degeneracy between initial non-Gaussianity and the effects of galaxy bias. The Gaussianity of initial conditions is much better tested on very large scales by the cosmic microwave background (CMB). A careful analysis of the COBE data has led to a detection of small non-Gaussianity (Ferreira, Magueijo & Gorski 1998), which is likely to be an instrumental effect (Bromley & Tegmark 1999; Banday, Zaroubi & Gorski 1999; Contaldi et al. 1999). Future measurements of Boomerang, MAP and PLANCK will either detect non-Gaussianity or strengthen the limits on it. Such possible non-Gaussian features are anyway small. With plausible extrapolation, they are likely to remain considerably smaller, at the $\sim 10 h^{-1}$ Mpc scale, than the signal that galaxy bias can induce in a reconstruction scheme as the one presented here (see Verde et al. 1999). As a consequence, the statistics of the reconstructed initial conditions can be used to give new valuable constraints on galaxy bias models, once the Gaussianity of initial conditions is either assumed or tightly constrained by the future CMB measurements.

The mildly non-linear evolution of the matter field is well modeled by the Zel'dovich (1970) approximation. It describes the evolution of the growing mode of perturbations into the non-linear regime, as long as the flow is still laminar. This restriction to the growing-mode dynamics gives an advantage over a backward N-body simulation, in which noise is amplified as a decaying mode. An inversion of the Zel'dovich mapping was proposed by Nusser & Dekel (1992). Their 'time machine' code requires the velocity potential field in real-space as an input. When applied to a galaxy catalogue, the initial conditions are not self-consistently obtained from the observed quantity, i.e. the galaxy density field in redshift space. Other methods for reconstructing the initial conditions, related to that of Nusser & Dekel (1992), were proposed by Gramann (1993) and Taylor & Rowan-Robinson (1993). Croft & Gataña (1997) developed PIZA, a method based on the least-action principle (Peebles 1989) and the Zel'dovich approximation. The same least-action principle has been exploited to construct efficient reconstruction algorithms by Nusser & Branchini (1999) and by Golberg and Spergel (1999). Weinberg (1992) and Narayanan & Weinberg (1998) imposed Gaussianity of the recovered initial conditions to improve the performance of a reconstruction algorithm applied to evolved Gaussian fields. Narayanan & Croft (1999) compared the performance of different reconstruction algorithms to N-body simulations. According to them, the most accurate

reconstruction schemes are that of Narayanan & Weinberg (1998) and PIZA.

The correctness of the reconstruction of the initial conditions relies on the accuracy of the input galaxy sample, and on the extent of the sampled volume. In this regard, the uniformity of the galaxy selection and the sky coverage are critical aspects. For this reason, the galaxy samples used to construct the galaxy density field have been selected from the objects contained in the all-sky point source catalogue (PSC) of the IRAS satellite, because they are observed on the whole sky by the same instrument, and IR-selected samples are less affected by dust extinction due to the Galactic Plane (although good all-sky optical catalogues as the ORS (Santiago et al. 1995) or the NOG (Marinoni et al. 1999) are now available). The far-IR selection is biased against spheroidal objects, so that IRAS galaxies tend to miss rich structures (even though at scales larger than $\sim 5 h^{-1}$ Mpc this effect is small, see Baker et al. 1999). The QDOT redshift catalogue (Lawrence et al. 1999) was defined by sparsely sampling the PSC galactic objects with 60μ flux larger than 0.6 Jy (the completeness limit). Fisher et al. (1995) defined their sample by limiting the PSC to a 60μ flux of 1.2 Jy. More recently, a redshift catalogue of all the PSC galaxies (hereafter PSCz; Saunders et al. 2000) has been completed. This catalogue provides the best presently available sample to quantify the galaxy density field of our local Universe.

To reconstruct the initial conditions of our local Universe, Nusser, Dekel & Yahil (1995) used the real-space density field of Yahil et al. (1991), obtained from the IRAS 1.2 Jy redshift catalogue, smoothed with a Gaussian filter of width $10 h^{-1}$ Mpc, using an iterative technique based on linear theory. The peculiar velocity potential, obtained from the real-space density field by means of an average non-linear velocity-density relation, was given as an input to the Nusser & Dekel's (1992) time machine. The 1-point probability distribution function (hereafter PDF) of their recovered initial conditions was consistent with a Gaussian. A reconstruction of the initial conditions was performed also by Kolatt et al. (1996), using the 1.2 Jy catalogue, and Narayanan et al. (1999), using the PSCz catalogue. In both papers the Gaussianity of the initial conditions was not found from data but forced, following the Gaussianization technique of Weinberg (1992) or Narayanan & Weinberg (1999). The recovered initial conditions were used to run N-body simulations to construct mock peculiar velocity catalogues (Kolatt et al. 1996) or to study the effect of biased galaxy formation in the reconstruction (Narayanan et al. 1999).

Monaco & Efstathiou (1999, hereafter ME99) have recently described an algorithm (ZTRACE) for recovering the real-space density field, the peculiar velocities and the initial conditions from a redshift catalogue with known selection function. ZTRACE is based on a self-consistent solution of the Zel'dovich approximation: it finds, with an iterative scheme, the set of initial conditions which evolve into the observed redshift-space density field, under the assumption that galaxies trace mass. The algorithm has been tested using N-body simulations. When the density field is smoothed with a mass-preserving adaptive scheme, the initial conditions and their PDF are reconstructed in an unbiased way, with the exception of the high peaks whose density contrast, linearly extrapolated to the present time, is $\gtrsim 1$. These have

already gone into the highly non-linear regime. As shown by ME99, the quality of the reconstruction is almost independent of the assumed background cosmology.

In this paper we apply the ZTRACE algorithm to the PSCz catalogue. In this way we recover the initial conditions of our local Universe on scales as small as $\sim 5 h^{-1}$ Mpc, thus pushing the reconstruction to the limit beyond which high non-linearity prevents any recovery. Here we focus on the reconstructed PDF of the initial conditions, testing its Gaussian shape; future work will address the use of the reconstructed initial conditions to simulate our local Universe. Section 2 describes the PSCz catalogue and the construction of the redshift-space density field. Section 3 gives a brief description of ZTRACE, and describes the results of its application to the PSCz catalogue. In Section 4 we analyze some sources of bias in the reconstructed initial PDF, namely the high-density tail, the effect of galaxy bias and the errors in the selection function. Section 5 describes the reconstructed initial PDF of the PSCz catalogue, and Section 6 gives the conclusions.

Throughout this paper distances are given in h^{-1} Mpc, with $h = H_0/(100 \text{ km/s/Mpc})$.

2 THE PSCZ CATALOGUE

For this analysis we use the recently completed PSCz catalogue, which is described in detail in Saunders et al. (2000). The catalogue is based on the IRAS PSC (Joint IRAS Science Working Group 1988), and comprises all galaxies with 60μ fluxes > 0.6 Jy. As the PSC is not complete to 0.6 Jy in 2HCON areas (Beichman et al. 1988), the 1HCON detections recovered from the PSC Reject file were added to the catalogue. Stars, other galactic sources and AGNs were eliminated by means of colour criteria, while residual contamination was eliminated by a combination of optical identifications, examination of the raw IRAS addscan profiles, examination of the Simbad database and, where still unclear, spectroscopic analysis. Redshifts for ~ 4600 galaxies not belonging to the QDOT (Lawrence et al. 1999) or the 1.2 Jy (Fisher et al. 1995) surveys, and not available in literature, were observed with several telescopes. Faint galaxies, with $B_J > 19.5$, were not observed; most of these objects are galaxies with $z > 0.1$, and their omission is irrelevant for the present analysis.

The final catalogue is 98 percent complete in redshift over 84 percent of the sky. The missing zones are the Galactic Plane (where the extinction is $A_V > 1.42$ mag), the areas covered by the LMC and SMC, and two small strips not observed by IRAS. Fig. 1 shows the Aitoff projected catalogue, with the uncovered zones masked in grey. The PSCz catalogue has already been used in other works on the topology of the large-scale structure (Canavezes et al. 1998), on the cosmological dipole (Rowan-Robinson et al. 1999; Schmoldt et al. 1999a), on the beta parameter (Schmoldt et al. 1999b), on the power spectrum of fluctuations (Sutherland et al. 1999), on the redshift distortions (Tadros et al. 1999) and on the peculiar velocity field (Branchini et al. 1999). Comparisons with other galaxy and galaxy cluster catalogues were presented by Seaborne et al. (1999) and Plionis et al. (1999). Reconstruction analyses were presented by Sharpe

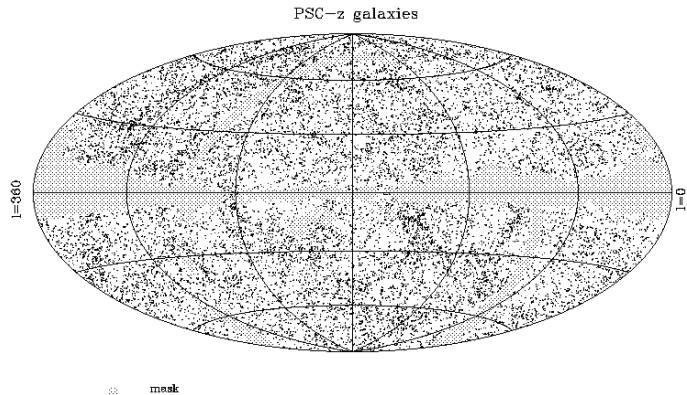


Figure 1. The PSCz catalogue in galactic coordinates. The regions uncovered by the IRAS PSC are masked in grey.

et al. (2000), based on the least-action principle, and by the already mentioned paper by Narayanan et al. (1999).

To calculate the galaxy density field from the PSCz catalogue it is necessary to know the selection function, which gives the number density of objects bright enough to be included in the catalogue, as a function of distance. The selection function is well fitted by the following functional form:

$$\Phi(r) = \Phi_* \frac{(r/r_*)^{1-\alpha}}{(1 + (r/r_*)^\gamma)^{\beta/\gamma}}, \quad (1)$$

where $r = cz/H_0$ is the redshift distance, but the volume is corrected for relativistic effects (assuming an Einstein-de Sitter Universe). As ZTRACE applies in a frame comoving with the background, we use redshifts in the CMB frame. A maximum likelihood fit, performed with the method of Mann, Saunders & Taylor (1996) and used in Saunders et al. (2000), gives the following best values for the parameters: $\Phi_* = 0.0224 h^3 \text{ Mpc}^{-3}$, $r_* = 64.10 h^{-1}$ Mpc, $\alpha = 1.41$, $\beta = 4.32$ and $\gamma = 1.39$. The resulting selection function is only marginally different from that calculated in the Local Group frame. The effects of uncertainties in the selection function will be addressed in Section 4.3.

3 APPLICATION OF ZTRACE TO THE PSCZ CATALOGUE

ZTRACE is based on a self-consistent solution of the Zel'dovich (1970) approximation. In the Lagrangian picture of fluid dynamics a mass element with initial (Lagrangian) comoving position \mathbf{q} is displaced to the final (Eulerian) position \mathbf{x} through a displacement field \mathbf{S} :

$$\mathbf{x}(\mathbf{q}, t) = \mathbf{q} + \mathbf{S}(\mathbf{q}, t). \quad (2)$$

The map \mathbf{S} is the dynamical variable in this approach. For small displacements, and for irrotational fluids, the first-

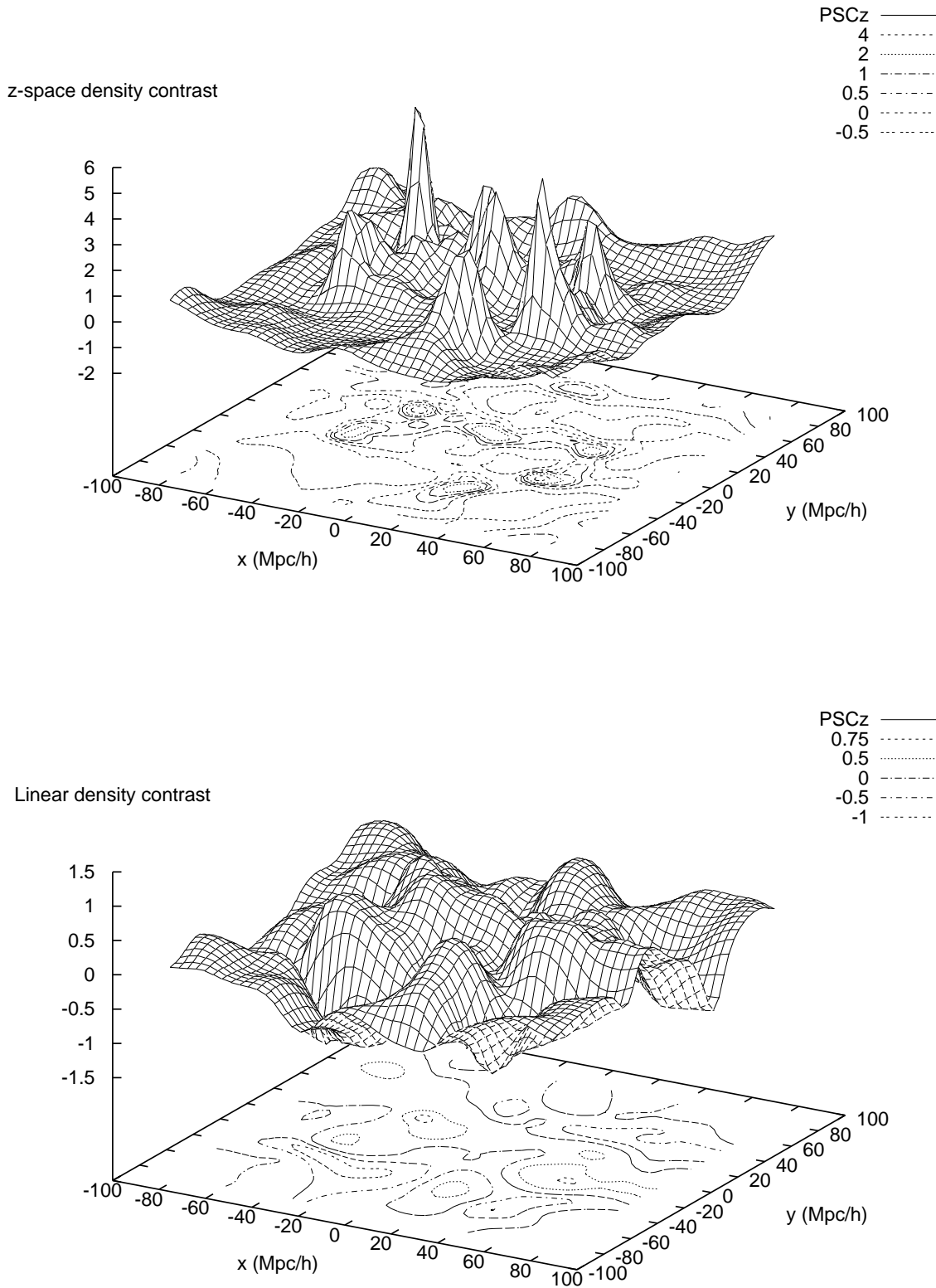


Figure 2. (a) Density field from the IRAS PSCz catalogue, adaptively smoothed over $7.6 h^{-1}$ Mpc within $80 h^{-1}$ Mpc. The Super-Galactic Plane is shown. The peaks correspond to well known superclusters; see text for details. (b) Initial density field, linearly extrapolated to the present time.

order growing mode gives the Zel'dovich (1970) approximation:

$$\mathbf{x}(\mathbf{q}, t) = \mathbf{q} - D(t)\nabla\varphi(\mathbf{q}). \quad (3)$$

Here $D(t)$ is the linear growing mode (see, e.g., Peebles 1980); for an Einstein-de Sitter universe it is equal to the scale factor $a(t)$. The growing mode is normalized so that $D(t_0) = 1$, where t_0 is the present time. $\varphi(\mathbf{q})$ is a rescaled version of the peculiar gravitational potential, such that, at an initial time t_i , $\nabla^2\varphi = \delta(\mathbf{q}, t_i)/D(t_i)$. The density contrast δ is defined as usual, $\delta(\mathbf{x}) = (\varrho(\mathbf{x}) - \bar{\varrho})/\bar{\varrho}$, where $\bar{\varrho}$ is the background density. It is useful to define the quantity:

$$\delta_i(\mathbf{q}) \equiv \delta(\mathbf{q}, t_i)/D(t_i). \quad (4)$$

δ_i is constant in linear theory, and is equal to the initial density contrast linearly rescaled to the present time. This quantity will be called the linear density contrast in the following.

In a redshift survey, the radial coordinate is the redshift distance, not the real distance. It is possible to generalize the Zel'dovich map, Eq. 3, to the redshift space \mathbf{s} :

$$\mathbf{s}(\mathbf{q}, t) = \mathbf{q} - D(t) [\nabla\varphi(\mathbf{q}) + f(\Omega) (\nabla\varphi(\mathbf{q}) \cdot \hat{\mathbf{x}}) \hat{\mathbf{x}}]. \quad (5)$$

Here $\hat{\mathbf{x}}$ is the versor of \mathbf{x} , and $f(\Omega) = d \ln D / d \ln a$ is usually approximated by $f(\Omega) \simeq \Omega^{0.6}$ (Peebles 1980), or by $f(\Omega, \Omega_\Lambda) \simeq \Omega^{0.6} + \Omega_\Lambda(1 + \Omega/2)/70$ (Lahav et al. 1991) if the cosmological constant is non-zero. Notice that the last term in the right-hand-side of Eq. 5 is the peculiar velocity along the line of sight.

The density contrast follows from the map in Eq. 3 or Eq. 5 through:

$$1 + \delta(\mathbf{q}) = [\det(\delta_{ab}^K + S_{a,b})]^{-1}. \quad (6)$$

Here δ_{ab}^K is the Kronecker tensor, and $S_{a,b}$ is the derivative of the map \mathbf{S} . ZTRACE is designed to invert the non-linear and non-local set of equations which connect the initial conditions to the redshift-space density, under the hypothesis of laminar flow, i.e. when the Zel'dovich map in redshift space, Eq. 5, is still single-valued. Multi-valued regions appear as soon as different mass elements which lie along the same line of sight are observed at the same redshift. This happens when the perturbation decouples from the Hubble flow, giving rise to multi-stream regions in the distance-redshift relation (often referred to as ‘‘triple-valued regions’’). The linear density contrast has a value of order one in such regions; ZTRACE is not able to reconstruct the high peaks of the density distribution.

ME99 describe in detail those techniques used to help the convergence of ZTRACE for smoothed density fields with standard deviations σ up to 0.7^* . The application of ZTRACE to the PSCz redshift catalogue can be summarized as follows.

(i) The masked regions are filled with a synthetic catalogue, so as to produce the galaxy density field over a large and connected spherical volume. We have used the procedure developed by Yahil et al. (1991) as modified by Branchini et al. (1999). According to this procedure, the zone of

avoidance of the Galactic disk, with galactic latitude $|b| < 8$ degrees, is divided in longitude and redshift bins. The galaxy number density in each bin is obtained by interpolating between those of the two 8 degree stripes above and below the bin. A synthetic galaxy catalogue is then obtained by randomly sampling the density field within the bins. In this way, the radial distribution follows the same PSCz selection function. The other masked regions of the sky which are outside the zone of avoidance are filled at random, according to the PSCz selection function. This algorithm is considered a better guess with respect to filling at random the masked regions, as it tends not to break the coherent structures, such as the Perseus-Pisces supercluster, which happen to cross the Galactic Plane. As a further test, we have also applied the lognormal interpolation procedure described in Saunders et al. (1999); the results are very similar and are not described here. The reconstruction method is robust with respect to the interpolation algorithm because only a small fraction of the sky is masked.

(ii) The relaxed groups are collapsed into spheroids. The effects of the highly non-linear dynamics are apparent in the redshift space as elongated structures along the line of sight, often referred to as ‘fingers of God’. As pointed out by Gramann, Cen & Gott (1994), a reconstruction scheme improves if such non-linear structures are collapsed before application of the algorithm. In ME99 the collapsing procedure was found to give a modest increase in the performance of ZTRACE. Following ME99, we have found the groups in the PSCz catalogue by applying a standard friends-of-friends algorithm, with radial and tangential linking lengths of 3 and $0.5 h^{-1}$ Mpc.

(iii) The catalogue is smoothed to generate a density field in redshift space. The performance of ZTRACE improves considerably if the density field is obtained with an adaptive, mass-preserving filtering of the galaxy catalogue. This is similar to a smoothing in the Lagrangian space, and correctly takes into account that overdensities come from larger patches which have contracted, while the opposite is true for underdensities. Following ME99, we have constructed the redshift-space galaxy density field by smoothing the PSCz point distribution (with the addition of the synthetic catalogue to fill the masked regions) with the adaptive smoothing code of Springel et al. (1998). This code requires the definition of a reference smoothing radius, which corresponds to the case of null density contrast; the adaptive refinements are then performed so that the smoothing filter always contains the same number of objects. As in ME99, the reference smoothing radius R is held constant within a given distance D , to a value such that 10 galaxies are on average contained in the filter at that distance. At larger distances, the reference smoothing radius is increased according to the selection function, so that 10 galaxies are contained on average within the filter. In this way, the outer parts that are more and more severely smoothed are used by ZTRACE to give the external tides to the inner region.

The density field is calculated on a 64^3 grid of size $240 h^{-1}$ Mpc. Fig. 2a shows the obtained density field in Super-Galactic coordinates, in the case $R=7.6 h^{-1}$ Mpc within $D=80 h^{-1}$ Mpc; the severe smoothing of the outer regions is apparent. The high peaks in the density distribution correspond to well-known structures as the Local Supercluster [at the position $(x, y) \sim (0, 0)$], the Great At-

* The tests performed by ME99 are limited to $\sigma \leq 0.7$. Anyway, for larger σ -values the distortion on the positive tail of the initial PDF becomes very strong.

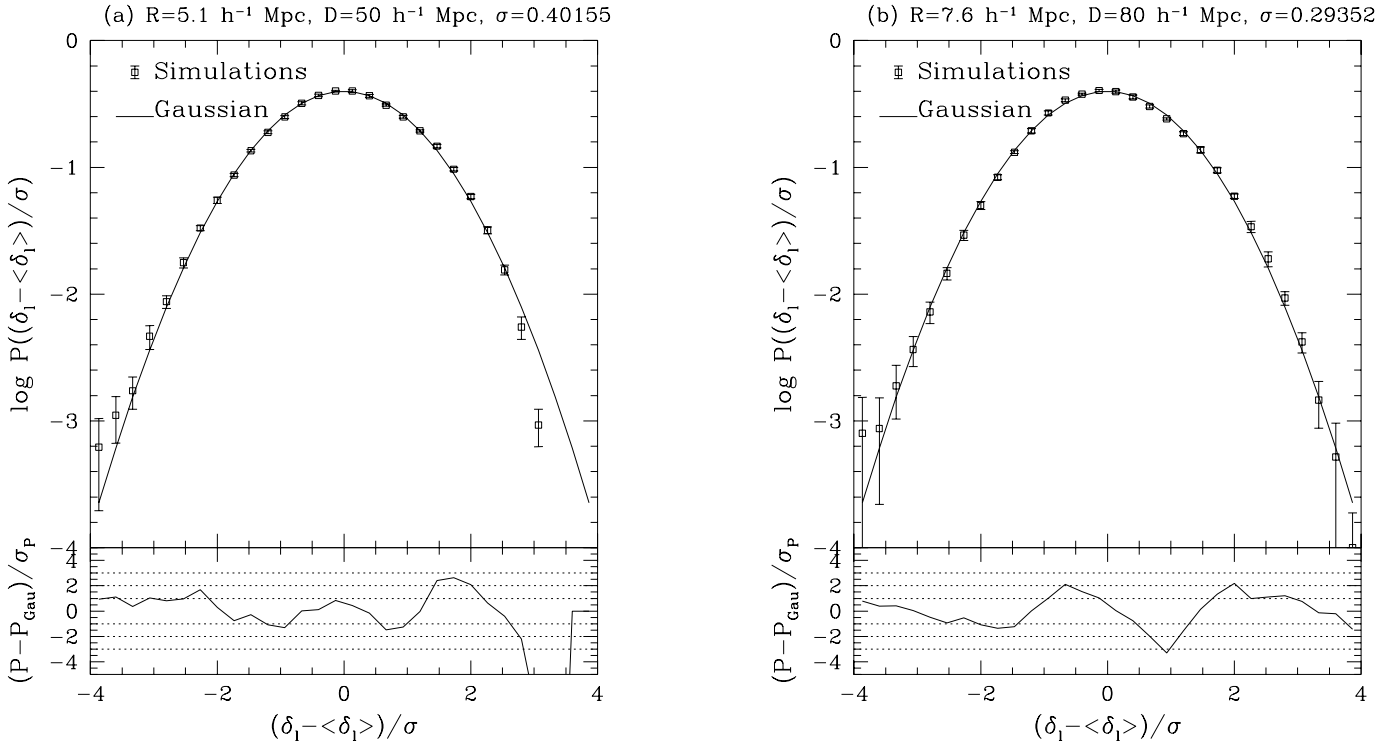


Figure 3. Reconstructed initial PDFs, averaged over 10 simulated catalogues. The errorbars shown are the square root of the variance of the mean among the realizations. The true Gaussian shape is also shown. (a) Smoothing $R = 5.1 h^{-1}$ Mpc within $D = 50 h^{-1}$ Mpc. (b) Smoothing $R = 7.6 h^{-1}$ Mpc within $D = 80 h^{-1}$ Mpc. The lower panels show the significance of the difference between the simulated and true initial PDFs. The lines at $\pm 1\sigma$, $\pm 2\sigma$ and $\pm 3\sigma$ are shown for clarity.

tractor region [the two peaks at $(x, y) \sim (-40, -20)$ and $(-40, 20)$], the Perseus-Pisces supercluster [the two peaks at $(x, y) \sim (20, -50)$ and $(40, -20)$] and its appendix beyond the Galactic Plane [the Camelopardalis supercluster, at $(x, y) \sim (60, 10)$], and the Coma supercluster [at $(x, y) \sim (0, 80)$] (see, e.g., Branchini et al. 1999).

(iv) The input density field is padded in the volume outside the largest inscribed sphere (of radius $120 h^{-1}$ Mpc), so as to have periodic boundary conditions. This is done so that we can apply FFT’s to solve the equations. ZTRACE is applied to the field; convergence is achieved within ~ 12 iterations. Fig. 2b shows the resulting initial conditions in the comoving real space (in terms of the linear density contrast δ_l , Eq. 4). (Notice that the linear density contrast is not bound to be ≥ -1). The main superclusters are originated from high peaks in the initial conditions. These peaks appear flattened because of the inability, discussed above, of ZTRACE to reconstruct the high-density regions. The different statistical properties of the initial conditions, with respect to the density field in real and redshift space, are apparent.

(v) The PDF of the initial conditions is calculated. In this analysis only the grid points within the distance D are considered. The points in the zone of avoidance ($|b| < 8^\circ$) are excluded, so as the central $10 h^{-1}$ Mpc sphere. This last exclusion is motivated by the inability of ZTRACE to converge in the neighborhood of the observer; the numerical solution tends to oscillate at the origin, where the map given in Eq. 5 is singular. To avoid this the density field is damped over $\sim 5 h^{-1}$ Mpc. The exclusion of the central region is not

a problem as its volume is small, and the PSCz is known to be incomplete at such small distances (Rowan-Robinson et al. 1991).

4 ERRORS AND BIASES IN THE RECONSTRUCTION OF THE INITIAL PDF.

The recovery of the initial PDF can be influenced by high non-linearities, by galaxy bias and by errors in the selection function. As shown in ME99, a wrong assumption on the background cosmology does not influence significantly the shape of the initial PDF.

4.1 The high-density tail

As mentioned above, ZTRACE is not able to recover the high peaks, which have decoupled from the Hubble flow. This induces a bias in the initial PDF, whose high density tail is suppressed. The underestimated high-density points influence the initial PDF also at moderate densities. It is useful to quantify this effect before addressing the Gaussian nature of the initial PDF reconstructed from the PSCz catalogue. To this aim, we have extracted mock PSCz catalogues from an N-body simulation of a standard CDM Universe (with $\Omega = 1$ and $\Gamma \equiv \Omega h = 0.5$) with normalization $\sigma_8 = 0.7$. The simulation, performed with the Hydra code (Couchman, Thomas & Pearce 1995), has already been presented in ME99. It is performed with 128^3 dark matter particles in a box of length $240 h^{-1}$ Mpc with a 256^3 base mesh

with adaptive refinements. As the volume used in the reconstruction is much smaller than the total volume of the simulation, it is convenient to extract more than one simulated PSCz catalogue from the simulation. We have extracted 10 catalogues, centred on random points, under the assumptions that galaxies trace mass and applying the PSCz selection function (in real space). It has been checked in ME99 that the selection in real space with a selection function determined in redshift space does not influence the result. The smoothing radius has been set to $R = 5.1 h^{-1}$ Mpc (constant within $D = 50 h^{-1}$ Mpc) or $R = 7.6 h^{-1}$ Mpc (constant within $D = 80 h^{-1}$ Mpc). When the smoothing is held constant within $D = 50 h^{-1}$ Mpc, the volume actually used in the reconstruction is 3.8 percent of the total volume of the simulation, so that the different realizations are accurately statistically independent. When the smoothing is held constant within $D = 80 h^{-1}$ Mpc, the volume used is 15.5 percent, and then the 10 realizations are oversampling the volume. This is approximately taken into account by calculating the variance among the various realizations as if they were $1/0.155 \simeq 6.45$ instead of 10.

For each simulated catalogue, the galaxies in the PSCz masked area are removed, then replaced using the same algorithm of Branchini et al. (1999) discussed above. We have checked that the masking procedure introduces noise but no bias in the reconstruction. The reconstruction proceeds as described in Section 3.

Because of sample variance, the reconstructed initial PDFs differ in general in mean ($\langle \delta_i \rangle$) and standard deviation (σ_i). To construct an average initial PDF it is then useful to consider the PDF of the quantity $(\delta_i - \langle \delta_i \rangle) / \sigma_i$. All the distributions are binned in the same way, and averages and variances are calculated for each bin. Fig. 3 shows the reconstructed initial PDFs, compared with the true Gaussian curve, for the two smoothing radii used. The upper panels show the reconstructed initial PDFs, the errors are the square root of the variance of the mean for the ten catalogues (calculated as if they were 6.45 in the second case, see above). The lower panels show the significance of the difference between the reconstructed and true initial PDF. It is apparent that the true Gaussian shape is recovered accurately, except in the high-density tail.

4.2 The effect of galaxy bias.

The simulated galaxy catalogues are created and reconstructed assuming that galaxies trace mass. This may not be true in practice, as galaxies may be biased tracers of the underlying mass distribution. As mentioned in the Introduction, galaxy bias may induce non-Gaussian distortions in the initial PDF, when this is reconstructed simply assuming that galaxies trace mass. To quantify this effect, it is convenient to apply ZTRACE, under the assumption that galaxies trace mass, to biased galaxy catalogues that are simulated assuming some specific bias model.

We have used a (deterministic, i.e. non-stochastic) power-law local bias scheme, already suggested, e.g., by Nusser et al. (1995) and by Lahav & Dekel (1999):

$$1 + \delta_g(\mathbf{x}) = (1 + b_0)(1 + \delta(\mathbf{x}))^{b_1}. \quad (7)$$

Here δ_g is the galaxy density contrast. This scheme respects the condition $\delta_g > -1$. For small density values this scheme

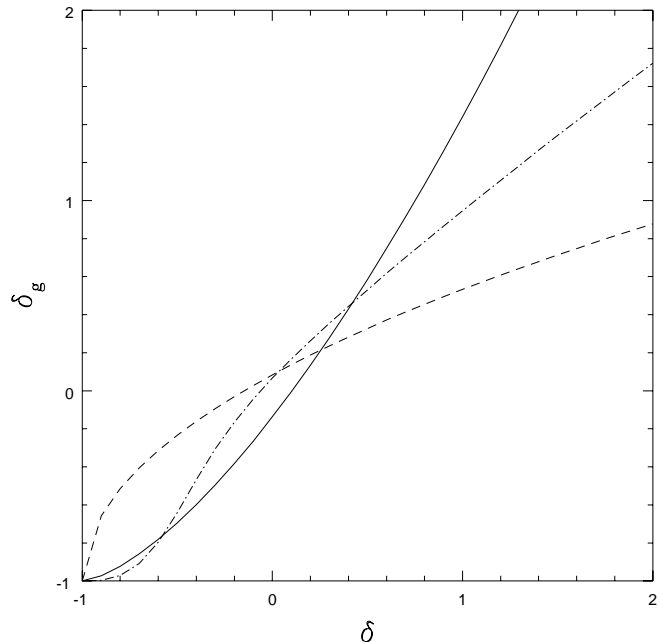


Figure 4. Bias functions used in the paper. Dashed line: anti-biased power-law with $b_1 = 0.5$. Continuous line: biased power-law with $b_1 = 1.5$. Dot-Dashed line: semi-analytical bias.

reduces to the linear bias, $\delta_g = (1 + b_0)b_1\delta$. b_0 is constrained so that $\langle \delta_g \rangle = 0$. In the following we will consider the anti-biased case $b_1 = 0.5$ and $b_0 = 0.084$, and the biased case $b_1 = 1.5$, and $b_0 = -0.137$. Fig. 4 shows the two bias curves.

A more physically motivated bias scheme can be obtained by using semi-analytic galaxy formation models (see, e.g., Benson et al. 1999; Somerville et al. 1999). In these models, the assembly of dark matter halos is described by means of N-body simulations, while the physics of the baryonic component is inserted in the halos through a set of simple analytic rules. Galaxy bias can then be obtained by comparing the density of galaxies with the density of dark matter. Narayanan et al. (1999) give an approximate bias function for the IRAS-like galaxies of Benson et al. (1999):

$$1 + \delta_g(\mathbf{x}) = A(1 + \delta(\mathbf{x}))^\alpha [C + (1 + \delta(\mathbf{x}))^{(\alpha-\beta)/\gamma}]^{-\gamma}. \quad (8)$$

Here $\alpha = 2.9$ and $\beta = 0.825$ are the asymptotic logarithmic slopes at small and large densities, while $A = 1.1$, $C = 0.08$ and $\gamma = 0.4$. This bias function is shown in Fig. 4. Compared to the simple power-law curves, it behaves as in the biased case in underdensities, but it is qualitatively more similar to the unbiased case in overdensities. We use the semi-analytic bias scheme as an exercise to quantify the distortion of the initial PDF expected from a more sophisticated bias function. It must be noticed, however, that this bias function is relative to a flat Universe with $\Omega_\Lambda = 0.7$ and $\sigma_8 = 0.9$, and to a density field smoothed with a top-hat filter with radius $3 h^{-1}$ Mpc, while we are applying it to an Einstein-de Sitter universe and to a density field Gaussian smoothed over $5 h^{-1}$ Mpc.

Following the same procedure as in Section 4.1, we have simulated three sets of 10 catalogues, with the three bias functions discussed above and shown in Fig. 4. The

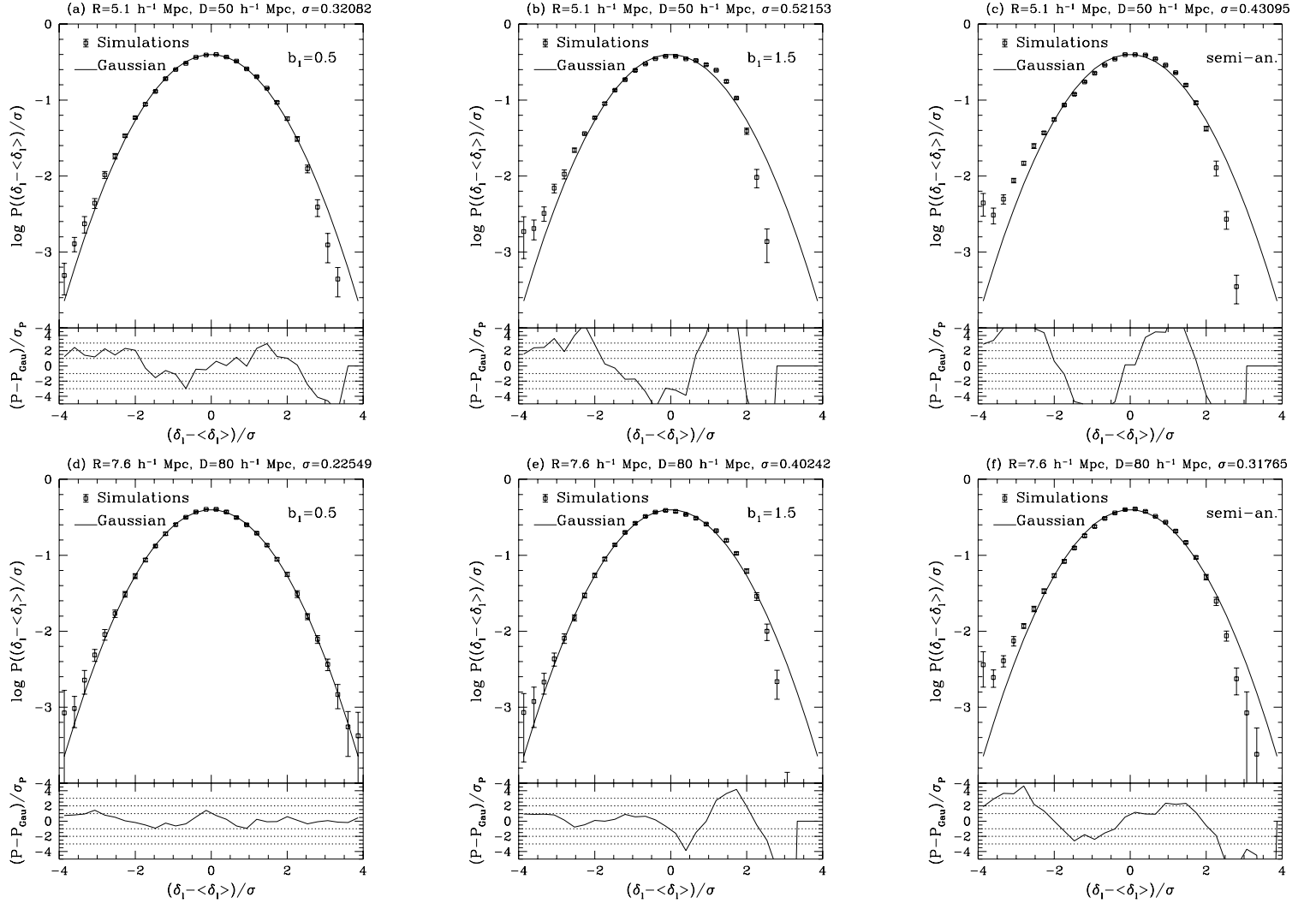


Figure 5. As in Fig. 3: reconstructed initial PDFs, averaged over 10 simulated catalogues, for biased catalogues, with $b_1 = 0.5$ (a,d), $b_1 = 1.5$ (b,e) or semi-analytic bias (c,f). The smoothing radius is set to $R = 5.1 h^{-1}$ Mpc within $D = 50 h^{-1}$ Mpc (a,b,c) or $R = 7.6 h^{-1}$ Mpc within $D = 80 h^{-1}$ Mpc (d,e,f).

bias schemes are applied to the real-space density field of the simulation, smoothed with a Gaussian filter of width $5 h^{-1}$ Mpc. Fig. 5. shows the obtained average initial PDFs; they are to be compared to those shown in Fig. 3. The Gaussian initial PDF is again well reconstructed in the “anti-biased” power-law case in which $b_1 = 0.5$, even though the low-density tail shows a $2\text{-}\sigma$ discrepancy when $R = 5.1 h^{-1}$ Mpc. In the “biased” power-law case, that in which $b_1 = 1.5$ and especially the semi-analytic case, significant distortions are apparent. For $R = 5.1 h^{-1}$ Mpc, the tail at low densities is overestimated, a dip and a bump are present respectively at $\delta_i/\sigma \sim 0$ and 1.5 . The same features are still present in the case $R = 7.6$, although they are less significant.

Fig. 5 shows that the application of ZTRACE with the no-bias assumption can lead to small but significant distortions in the reconstructed initial PDF. However, these distortions are revealed by averaging over ten realizations of the PSCz catalogue, but they are not statistically significant for single biased realizations. The PSCz survey is not

large enough to reveal such deviations, but larger surveys such as the 2dF and SDSS surveys may be able to provide constraints on non-linear bias schemes. Of course this conclusion may change if stronger bias functions are considered; however, evidence on IRAS galaxies suggests that they are weakly biased with respect to the matter density (see, e.g., Saunders et al. 1999).

4.3 Errors in the selection function

Another potential source of distortion on the initial PDF comes from errors in the selection function. Given the highly correlated nature of the density field, a systematic error in the density estimate in a spherical shell which happens to contain some large voids or clusters can influence the shape of the initial PDF. To test for this, we have collected the selection functions (in the Local Group frame) used by ME99, Sutherland et al. (1999), Canavezes et al. (1998), Branchini et al. (1999), and Springel (1996). We have added to these our own determination of the selection function in the Local

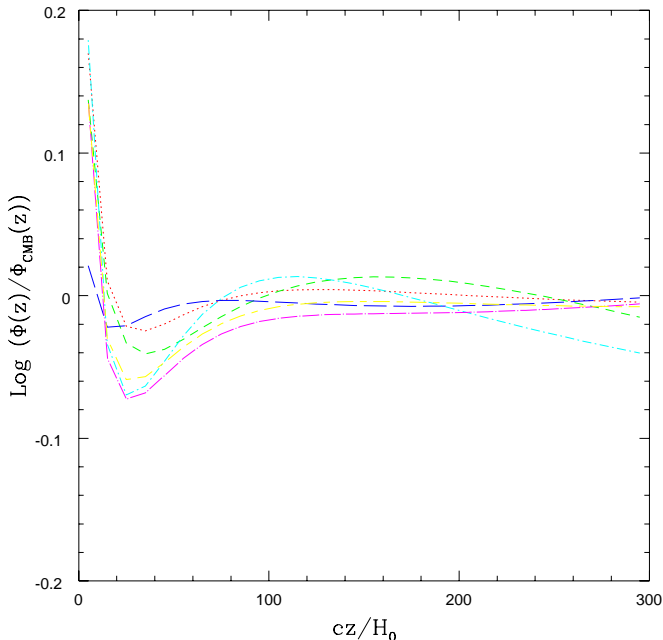


Figure 6. Residuals of the selection functions taken from ME99 (long-dashed), Sutherland et al. (1999) (dashed), Branchini et al. (1999) (dot-dashed), Canavezes et al. (1999) (dot-long dashed), Springel (1996) (short-long dashed), and determined by us in the Local Group frame (dotted), with respect to the one calculated by us in the CMB frame.

Group frame, performed as described in Section 2. The differences between the various functions, which are of order of 10 percent, are due to the slightly different versions of the catalogue and mask used by the various authors, and to differences in the fitting procedure. Fig. 6 shows the residuals of these selection functions with respect to the one used in this paper (Eq. 1). Notice that all the residuals show the same systematics because the selection functions are relative to the Local Group frame. Then, the effect of errors in the selection function is overestimated in this analysis.

The first simulated PSCz catalogue (with no bias) has been reconstructed assuming either the correct or one of the six other selection functions listed above. Fig. 7 shows the seven reconstructed initial PDFs, compared with the average reconstructed initial PDF already shown in Fig. 3. Differently from Fig. 3, the errors shown are the (square root of the) variance between the various realizations (instead of the variance of the mean). This is the correct error to use when assessing the difference between a single realization and the average initial PDF. Again, the lower panels show the significance of the disagreement. The various initial PDFs are hardly distinguishable, no significant distortion is induced. We conclude that the uncertainty in the selection function does not influence significantly the shape of the reconstructed initial PDF.

5 THE RECONSTRUCTED INITIAL PDF OF THE PSCZ CATALOGUE

The PSCz catalogue has been adaptively smoothed according to the smoothing strategy described in Section 3. The reference radius has been held constant, within $D = 50$ and $80 h^{-1}$ Mpc, to the values of $R = 5.1$ and $7.6 h^{-1}$ Mpc. Fig. 8 shows the reconstructed initial PDFs of the PSCz catalogue compared with the results of the simulated catalogues described in Section 3.1 (with no bias and CMB selection function) and shown in Fig. 3. The error associated to the simulated initial PDFs is the square root of the variance between the realizations.

The value of σ_8 for the PSCz density field turns out to be about 0.8 (Sutherland et al. 1999; Seaborne et al. 1999), slightly larger than the value 0.7 used in our test simulation. As a consequence, the variance of the reconstructed initial PDF is slightly larger than the test one smoothed with the same radius. This has some effect on the spurious high-density cutoff of the PDF induced by ZTRACE. To compare reconstructed PDFs that have roughly the same variance, the PSCz has been smoothed over $R = 7.2$ and $10.1 h^{-1}$ Mpc within $D = 75$ and $105 h^{-1}$ Mpc. Fig. 9 shows the comparison with the same PDFs of simulated catalogues as in Fig. 3 and 8.

The reconstructed initial PDF of the PSCz catalogue disagrees significantly with the simulated one in Fig. 8a (smoothing radius $R = 5.1 h^{-1}$ Mpc), where the standard deviation σ of the two PDFs that are compared are different. Even in this case, significant distortions are visible only on the positive-density side, for $(\delta_i - \langle \delta_i \rangle) / \sigma \gtrsim 1$. In this range of densities the influence of the high-density cut (which is different in the two cases due to the difference in σ) is strong. This discrepancy vanishes in Fig. 9a, when comparing the reconstructed PDFs of simulated and PSCz catalogues with similar variances. Besides, the distortions on the negative-density side, where we expect to find the signature of galaxy bias (see Fig. 4), are never significant, except a $3\text{-}\sigma$ discrepancy which is limited to one single bin. Figs. 8b and 9b show the same comparison for the larger smoothing radii. In this case, no strongly significant distortions are visible, although some modest but persistent discrepancy at the $3\text{-}\sigma$ level is present both on the positive- and on the negative-density sides.

We conclude that there is no convincing evidence for non-Gaussianity in the initial PDF reconstructed from the PSCz catalogue. Notably, the overall pattern of the residuals is similar to the distortions induced by biased power-law or semi-analytic bias. Anyway, the statistical significance of these distortions is too marginal to draw any conclusion.

The Gaussianity of the reconstructed initial PDF gives support to the hypotheses of Gaussianity of initial conditions and of modest bias of IRAS objects (as described in Section 4.2). In particular, the low-density tail of the initial PDF remains Gaussian down to fluctuations of ~ 2.5 times the standard deviation. The fact that ‘the voids are too devoid’ of bright galaxies has often been seen as a possible problem for CDM-like models of structure formation (see, e.g., Peebles 1999). The result presented here shows that the voids, as defined by IRAS galaxies, are as underdense as they are expected to be as an effect of gravitation, at least

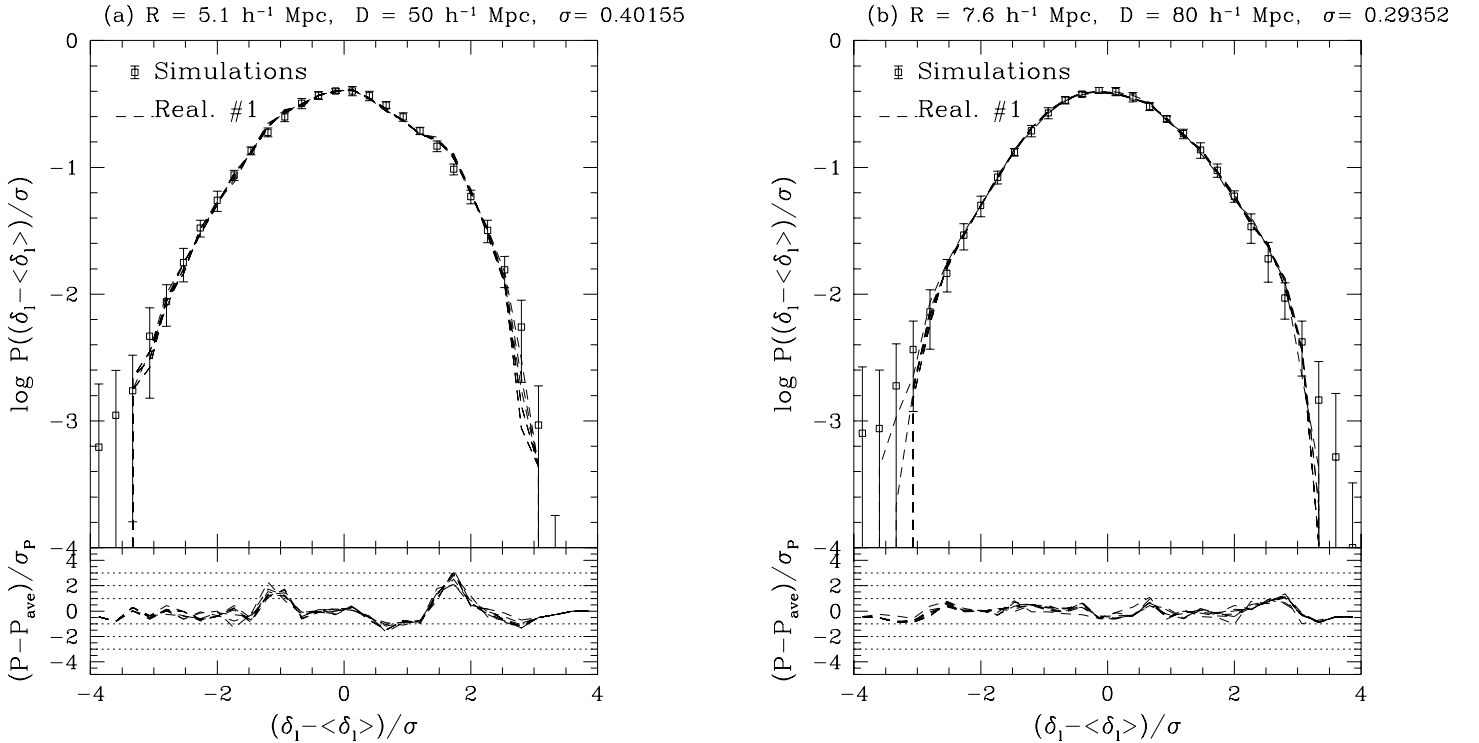


Figure 7. Reconstructed initial PDF for the first simulated (unbiased) catalogue, compared to the average simulated initial PDF of Fig. 3. The density field is reconstructed using either the correct selection function or one of the six alternatives listed in the text. The error associated to the simulated initial PDFs is the square root of the variance among the realizations. The lower panels show the significance of the disagreement between the given realization and the average.

on scales as small as $5 h^{-1}$ Mpc, where the highly non-linear regime is still not dominant.

6 SUMMARY AND CONCLUSIONS

The ZTRACE algorithm has been applied to the new IRAS PSCz redshift catalogue to reconstruct the initial conditions of our local Universe. The ZTRACE algorithm, recently proposed by ME99, is known to give an unbiased estimate of the initial density which generates, through gravitational collapse in the Zel’dovich (1970) approximation, the observed galaxy density field in the redshift space under the assumption that galaxies trace mass. The reconstructed initial conditions of our local Universe can be used as input to N-body simulations, with the small-scale modes restored with a Monte-Carlo procedure (Kolatt et al. 1996; Narayanan et al. 1999).

The results presented in this paper push the reconstruction of initial conditions to scales of $5 h^{-1}$ Mpc. This is close to the limit at which highly non-linear dynamics becomes dominant, hampering any detailed inversion of the gravitational evolution. This paper improves by a factor of two in scale over the previous determination of the initial PDF, by Nusser et al. (1995). This improvement is due to the increased sampling density and depth of the new PSCz catalogue relative to previous IRAS-based catalogues such as QDOT (Lawrence et al. 1999) or 1.2 Jy Fisher et al. (1995), and to the superior performance of ZTRACE, com-

pared to previous reconstruction algorithms (see ME99 and Narayanan & Croft 1999).

The reconstructed initial PDF of the local Universe is Gaussian to within the accuracy of the method. The lack of detection of non-Gaussianity in the initial PDF supports the hypothesis that initial conditions are Gaussian and IRAS galaxies are not strongly biased with respect to the matter density. Moreover, it shows that the voids are as devoid of bright galaxies as they should be as an effect of gravity (see, e.g., Peebles 1999). The Gaussian nature of the primordial perturbations has been tested on much larger scales and with greater accuracy by measurements of the CMB. Then this result, besides offering a complementary support for Gaussianity on the scale of $\sim 5\text{--}10 h^{-1}$ Mpc, gives original constraints on the nature of galaxy bias, which in general induces distortions on the initial PDF reconstructed under the no-bias hypothesis. However, our tests show that the distortion induced by realistic power-law galaxy bias models, especially on the low-density tail, is just beyond the reach of the PSCz catalogue. Future surveys, like the 2dF or the SDSS, covering larger volume than PSCz, will provide a way to constrain galaxy bias beyond the linear level from the reconstruction of the initial PDF.

ACKNOWLEDGMENTS

The Hydra team (H. Couchman, P. Thomas, F. Pearce) has provided the code for N-body simulations. Volker Springel has kindly provided a C version of the code for adaptive

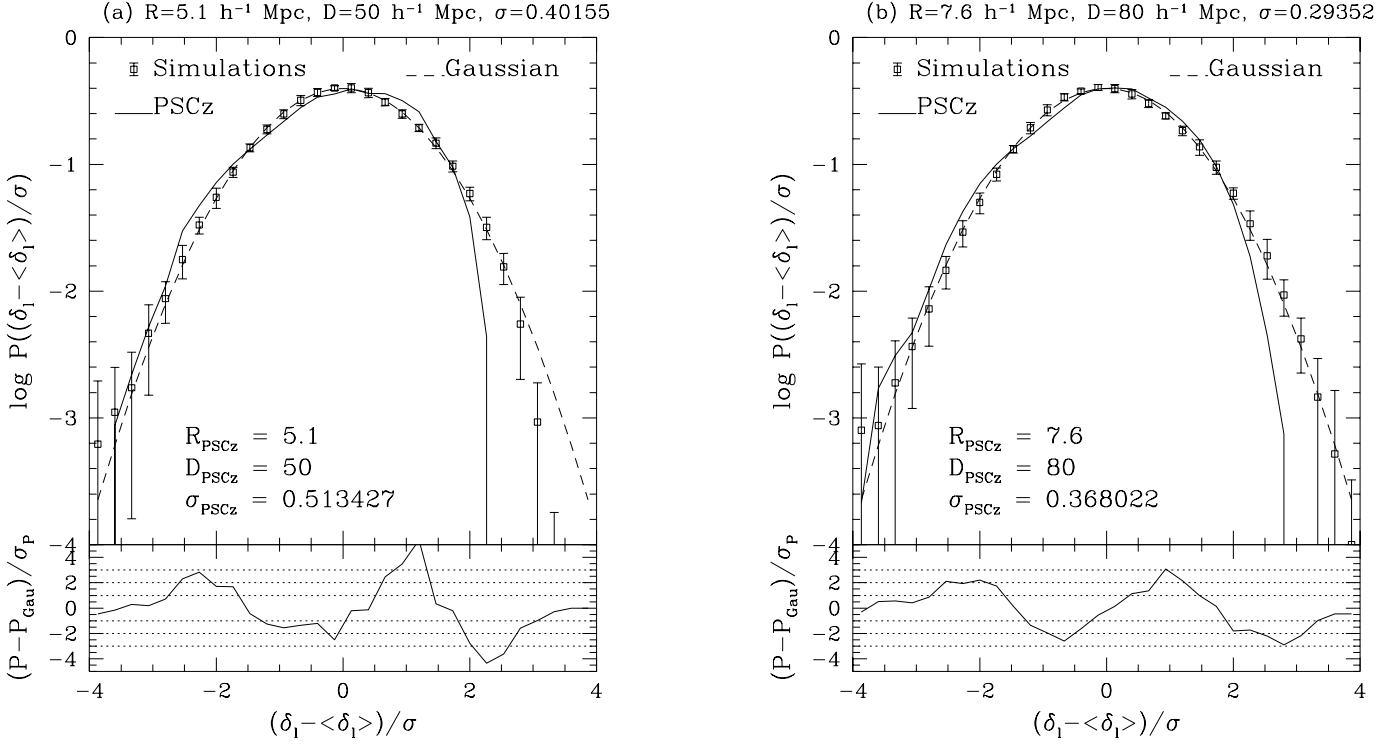


Figure 8. Reconstructed initial PDFs for the PSCz catalogue compared with those for the simulated catalogues. The smoothing radii are $R = 5.1$ and $7.6 \text{ h}^{-1} \text{ Mpc}$ within $D = 50$ and $80 \text{ h}^{-1} \text{ Mpc}$. The dashed Gaussian line is shown for reference. The lower panels show the significance of the disagreement.

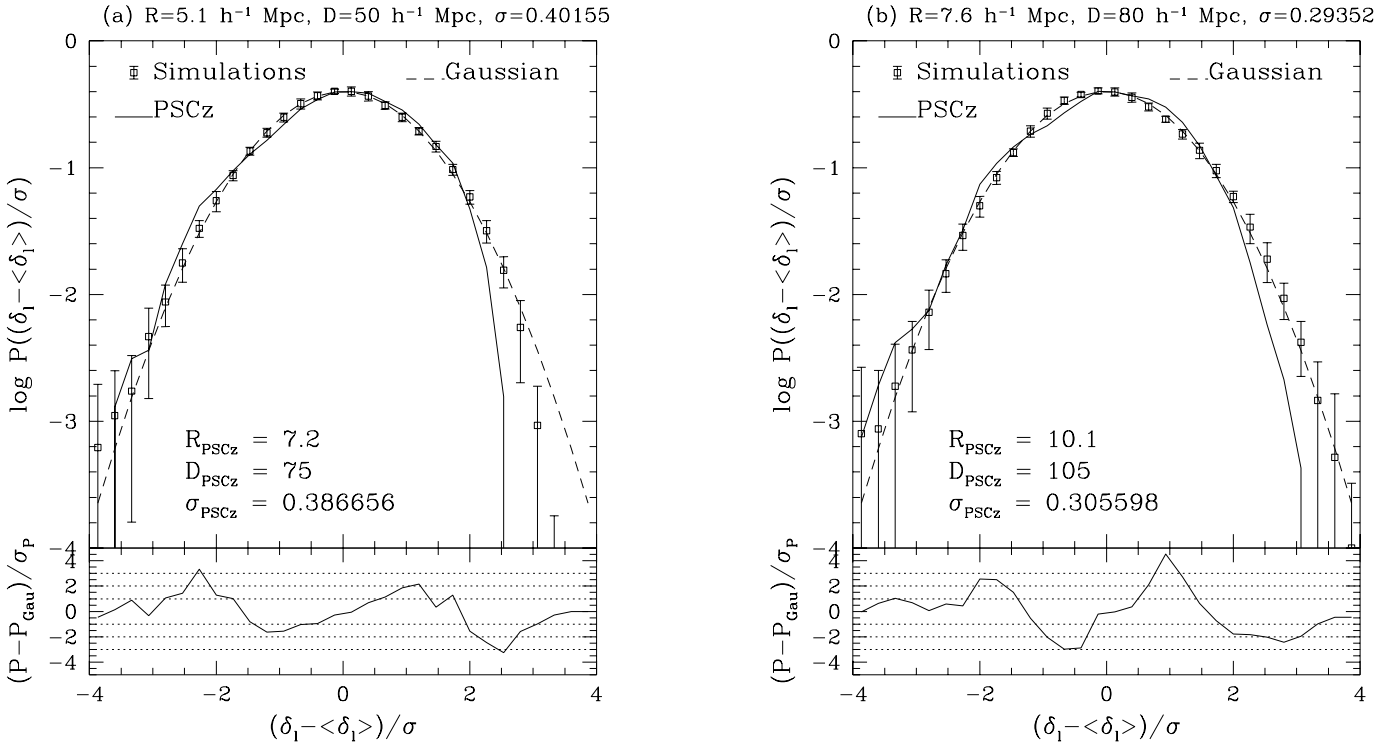


Figure 9. As in Fig. 8, but the PSCz catalogue is smoothed with $R = 7.2$ and $10.1 \text{ h}^{-1} \text{ Mpc}$ within $D = 75$ and $105 \text{ h}^{-1} \text{ Mpc}$. The smoothing radii are chosen so that the variances of the initial PDFs for PSCz and simulated catalogues roughly coincide.

smoothing. We thank the referee, David Weinberg, for his helpful comments. P.M. thanks Christian Marinoni and Inga Schmoldt for discussions. P.M. has been supported by the EC TMR Marie Curie grant ERB FMB ICT961709.

REFERENCES

- Banday A.J., Zaroubi S., Gorski K.M., 1999, ApJ, in press (astro-ph/9908070)
- Baker J.E., Davis M., Strauss M.A., Lahav O., Santiago B.X., 1998, ApJ, 508, 6
- Beichman C., Habling G.N., Clegg P.E., Chester T.J., 1988, IRAS Explanatory Supplement, NASA RP-1190, Vol 1, US Government Printing Office, Washington DC
- Benson A.J., Cole S., Frenk C.S., Baugh C.M., Lacey C.G., 1999, MNRAS, submitted (astro-ph/9903343)
- Branchini E., Teodoro L., Frenk C.S., Schmoldt I., Efstathiou G.P., White S.D.M., Saunders W., Rowan-Robinson M., Keeble O., Tadros H., Maddox S.J., Oliver S., Sutherland W., 1999, MNRAS, 308, 1
- Brandenberger R.H., 1998, Pramana 51, 191 (hep-ph/9806473)
- Bromley B. C., Tegmark M., 1999, ApJ, 524, L79
- Canavezes A., Springel V., Oliver S. J., Rowan-Robinson M., Keeble O., White S. D. M., Saunders W., Efstathiou G., Frenk C. S., McMahon R. G., Maddox S., Sutherland W., Tadros H., 1998, MNRAS, 297, 777
- Catelan P., Lucchin F., Matarrese S., Porciani C., 1998, MNRAS, 297, 692
- Contaldi C. R., Ferreira P. G., Magueijo J., Gorski K. M., submitted to ApJ (astro-ph/9910138)
- Couchman H., Thomas P., Pearce F., 1995, ApJ 452 797
- Croft R. A. C., Gaztañaga E., 1997, MNRAS, 285, 793
- Ferreira P.G., Magueijo J., Gorski K.M., 1998, ApJ, 503, L1
- Fisher K., Huchra J.P., Strauss M., Davis M., Yahil A., Schlegel D., 1995, ApJS, 100, 69
- Goldberg D.M., Spergel D.N., 1999, astro-ph/9912408
- Gramann M., 1993a, ApJ, 405, 449
- Gramann M., Cen R., Gott J. R., 1994, ApJ, 425, 382
- Joint IRAS Science Working Group, 1988, in IRAS Point Source Catalogue, Version 2, US Government Printing Office, Washington DC
- Kolatt T., Dekel A., Ganon G., Willick J. A., 1996, ApJ, 458 419
- Lahav O., Dekel A., 1999, ApJ, 520, 24
- Lahav O., Lilje P. B., Primack J. R., Rees M. J., 1991, MNRAS, 251, 128
- Lawrence A., Rowan-Robinson M., Ellis R.S., Frenk C.S., Efstathiou G.P., Kaiser N., Saunders W., Parry I.R., Xiaoyang Xia., Crawford J., 1999, MNRAS, 308, 897
- Linde A., 1990, Particle Physics and Inflationary Cosmology. Harwood Academic Publishers
- Mann R.G., Saunders W., Taylor A.N., 1996, MNRAS, 279, 636
- Marinoni C., Monaco P., Giuricin G., Costantini B., 1999, ApJ, 521, 50
- Monaco P., Efstathiou G., 1999, MNRAS, 308, 763 (ME99)
- Narayanan V. K., Croft R. A. C., 1999, ApJ, 515, 471
- Narayanan V. K., Weinberg D., 1998, ApJ, 508, 440
- Narayanan V. K., Weinberg D., Branchini E., Frenk C.S., Maddox S., Oliver S., Rowan-Robinson M., Saunders W., 1999, submitted to ApJ (astro-ph/9910229)
- Nusser A., Branchini E., 1999, MNRAS, submitted (astro-ph/9908167)
- Nusser A., Dekel A., 1992, ApJ, 391, 443
- Nusser A., Dekel A., Yahil A., 1995, ApJ, 449 439
- Pearce F.R., Jenkins A., Frenk C.S., Colberg J.M., White S.D.M., Thomas P.A., Couchman H.M.P., Peacock J.A., Efstathiou G., 1999, ApJ, 521, L99
- Peebles P. J. E., 1980, The Large Scale Structure of the Universe. Princeton Univ. Press
- Peebles P. J. E., 1989, ApJ, 344, L53
- Peebles P.J.E., 1999, in Clustering at High Redshift, Marseilles, eds. A. Mazure and O. Le Fevre, in press (astro-ph/9910234)
- Plionis M., Basilakos S., Rowan-Robinson M., Maddow S.J., Oliver S.J., Keeble O., Saunders W., 1999, MNRAS, in press (astro-ph/9912406)
- Rowan-Robinson M., Saunders W., Lawrence A., Leech K., 1991, MNRAS, 253, 485
- Rowan-Robinson M., Sharpe J., Oliver S. J., Keeble O., Canavezes A., Saunders W., Taylor A. N., Valentine H., Frenk C. S., Efstathiou G. P., McMahon R. G., White S. D. M., Sutherland W., Tadros H., Maddox S. J., 1999, MNRAS, in press (astro-ph/9912223)
- Salopek D.S., 1999, in COSMO-98, ed. D. Caldwell, PASP, in press (astro-ph/9903327)
- Santiago B.X., Strauss M.A., Lahav O., Davis M., Dressler A., Hucra J.P., 1995, ApJ, 446, 457
- Saunders W., et al., 1999, in 'Towards an Understanding of Cosmic Flows', eds S. Courteau, M. Strauss, J. Willick, PASP, in press (astro-ph/9909190)
- Saunders W., Sutherland W.J., Maddox S.J., Keeble O., Oliver A.J., Rowan-Robinson M., Mc Mahon R.G., Efstathiou G., Tadros H., White S.D.M., Frenk C.S., Carramiñana A., Hawkins M.R.S., 2000, MNRAS, in press (astro-ph/0001117)
- Schmoldt I., Branchini E., Teodoro L., Efstathiou G., Frenk C.S., Keeble O., McMahon R., Maddox S., Oliver S., Rowan-Robinson M., Saunders W., Sutherland W., Tadros H., White S.D.M., 1999a, MNRAS, 304, 893
- Schmoldt I., Saar V., Saha P., Branchini E., Efstathiou G., Frenk C.S., Keeble O., Maddox S., McMahon R., Oliver S., Rowan-Robinson M., Saunders W., Sutherland W.J., Tadros H., White S.D.M., 1999b, AJ, 118, 1146
- Seaborne M.D., Sutherland W., Tadros H., Efstathiou G.P., Frenk C.S., Keeble O., Maddox S., McMahon R.G., Oliver S., Rowan-Robinson M., Saunders W., White S.D.M., 1999, MNRAS, 309, 89
- Seljak U., 2000, PRD, submitted (astro-ph/0001493)
- Sharpe J., Rowan-Robinson M., Canavezes A., Saunders W., Efstathiou G., Frenk C.S., Keeble O., Mc Mahon R.G., Maddox S.J., Oliver S.J., Sutherland W., Tadros H., White S.D.M., 2000, MNRAS in press
- Sigad Y., Branchini E., Dekel A., 2000, ApJ, submitted (astro-ph/0002170)
- Somerville R.S., Lemson G., Sigad Y., Dekel A., Kauffmann G., White S.S.M., 1999, MNRAS, submitted (astro-ph/9912073)
- Springel V., 1996, Topology and Luminosity Function of the PSCz Redshift Survey, M.Sc. Thesis, Eberhard-Karls-Universität Tübingen
- Springel V., White S. D. M., Colberg J. M., Couchman H. M. P., Efstathiou G. p., Frenk C. S., Jenkins A. R., Pearce F. R., Nelson A. H., Peacock J. A., Thomas P. A., 1998, MNRAS, 298, 1169
- Sutherland W., Tadros H., Efstathiou G., Frenk C. S., Keeble O., Maddox S., McMahon R. G., Oliver S., Rowan-Robinson M., Saunders W., White S. D. M., 1999, MNRAS, 308, 289
- Tadros H., Ballinger W.E., Taylor A.N., Heavens A.F., Efstathiou G., Saunders W., Frenk C.S., Keeble O., McMahon R., Maddox S.J., Oliver S., Rowan-Robinson M., Sutherland W., White S.D.M., 1999, MNRAS, 305, 527
- Taylor A. N., Rowan-Robinson M., 1993, MNRAS, 265, 809
- Tegmark M., Peebles P.J.E., 1998, ApJ, 500, L79
- Verde L., Wang L., Heavens A.F., Kamionkowski M., 1999, MNRAS, submitted (astro-ph/9906301)
- Weinberg D. H., 1992, MNRAS, 254, 315
- Yahil A., Strauss M. A., Davis M., Hucra J. P., 1991, ApJ, 372, 380

Zel'dovich, Ya.B. 1970, *Astrofizika* 6, 319 (transl.: 1973, *Astrophysics* 6, 164)

This paper has been produced using the Royal Astronomical Society/Blackwell Science L^AT_EX style file.